

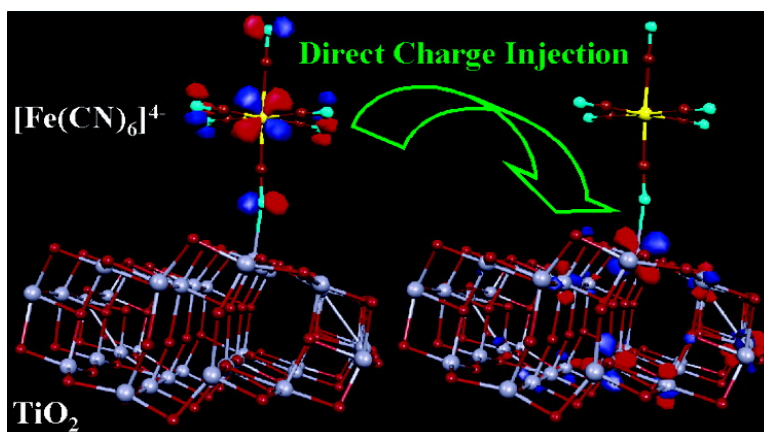
Communication

Time-Dependent DFT Study of [Fe(CN)₆] Sensitization of TiO₂ Nanoparticles

Filippo De Angelis, Antonio Tilocca, and Annabella Selloni

J. Am. Chem. Soc., **2004**, 126 (46), 15024-15025 • DOI: 10.1021/ja045152z • Publication Date (Web): 30 October 2004

Downloaded from <http://pubs.acs.org> on April 5, 2009



More About This Article

Additional resources and features associated with this article are available within the HTML version:

- Supporting Information
- Links to the 9 articles that cite this article, as of the time of this article download
- Access to high resolution figures
- Links to articles and content related to this article
- Copyright permission to reproduce figures and/or text from this article

[View the Full Text HTML](#)



ACS Publications
 High quality. High impact.

Time-Dependent DFT Study of $[\text{Fe}(\text{CN})_6]^{4-}$ Sensitization of TiO_2 Nanoparticles

Filippo De Angelis,^{*,†,‡} Antonio Tilocca,[‡] and Annabella Selloni[‡]

Istituto CNR di Scienze e Tecnologie Molecolari (ISTM), Dipartimento di Chimica, Università di Perugia, I-06213, Perugia, Italy, and Department of Chemistry, Princeton University, Princeton, New Jersey 08540

Received August 11, 2004; E-mail: filippo@thch.unipg.it

A key process in the operation of dye-sensitized photovoltaic solar cell devices is the charge injection from the dye molecule at the surface of the semiconductor nanoparticle to the conduction band states within the nanoparticle itself.¹ For Ru(II)-polypyridyl dyes, which are most commonly used in the Graetzel cells, the generally accepted injection mechanism involves photoexcitation to a dye excited state, from which an electron is subsequently transferred to the semiconductor, typically TiO_2 anatase, conduction band states.¹ By contrast, a mechanism involving a direct photoexcitation from the dye to an empty state of the nanoparticle is believed to occur for $[\text{Fe}(\text{CN})_6]^{4-}$ on TiO_2 .² This type of behavior is characterized by the appearance of an absorption band at energies below the onset of the semiconductor band-to-band transitions, and was assigned as a metal to particle charge transfer (MPCT) transition.² For the $[\text{Fe}(\text{CN})_6]^{4-}/\text{TiO}_2$ system in acetonitrile or aqueous solution, this band is found at 2.95 eV (420 nm),^{2,3} and, on the basis of electroabsorption spectroscopy data,³ the final state of the transition has been recently suggested to be localized on a small number of Ti(IV) atoms around the point where the dye is attached to the surface. A direct injection mechanism has been also proposed for catechol on TiO_2 , on the basis of semiempirical calculations.^{4a}

In this work we present density functional theory (DFT) and time-dependent DFT (TDDFT) calculations of the absorption spectrum of $[\text{Fe}(\text{CN})_6]^{4-}$ adsorbed on a TiO_2 anatase nanoparticle model, with the aim of providing a detailed description of the electronic structure of this prototype system and to understand the character of the states involved in the molecule \rightarrow semiconductor charge-transfer process. Previous theoretical studies of dyes adsorbed on TiO_2 were generally restricted to small organic molecules.⁴ First, we used a Car–Parrinello⁵ (CP) approach to optimize the structures of the TiO_2 nanoparticle model, the $[\text{Fe}(\text{CN})_6]^{4-}$ dye, and the interacting $[\text{Fe}(\text{CN})_6]^{4-}/\text{TiO}_2$ system. CP calculations were performed in a vacuum, using the PBE functional⁶ together with a plane-wave basis set and ultrasoft pseudopotentials.⁷ A stoichiometric anatase $\text{Ti}_{38}\text{O}_{76}$ cluster of nanometric dimensions exposing (101) surfaces, similar to that described in ref 4a, was employed to represent the nanoparticle, Figure 1. Next, the CP geometries were used for TDDFT calculations to determine the lowest excitation energies of the investigated systems. For these studies we used the Gaussian03 (G03) code,⁸ with the B3LYP functional⁹ and 6-311g* and 3-21g* basis sets¹⁰ on the $[\text{Fe}(\text{CN})_6]^{4-}$ and TiO_2 systems, respectively, for a total of 1972 basis functions. G03 calculations were performed in water solution, with solvation effects described by the non-equilibrium C-PCM method.¹¹ Since a TDDFT calculation on the $[\text{Fe}(\text{CN})_6]^{4-}/\text{TiO}_2$ system turned out to be practically unaffordable beyond the first 12 excitations, for this system the overall spectrum was finally computed using a simplified approach in which excitation energies are approximated by orbital

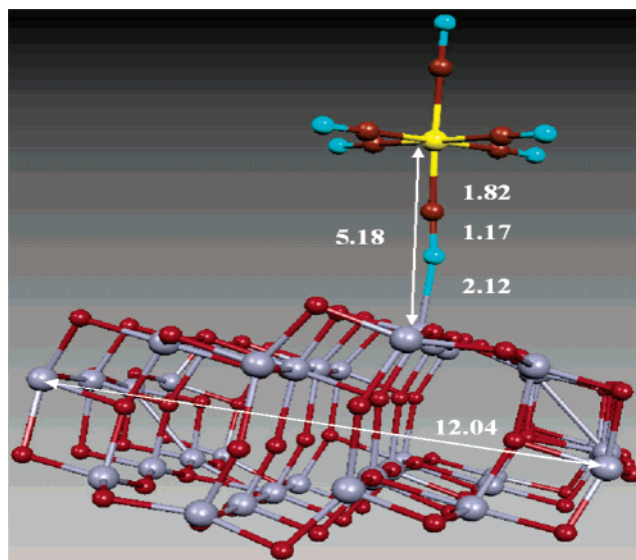


Figure 1. Optimized geometrical structure of the $[\text{Fe}(\text{CN})_6]^{4-}/\text{TiO}_2$ system in the monodentate configuration. Main bond distances (Å) are reported. Grey = Ti, red = O, turquoise = N, brown = C and yellow = Fe atoms.

energy differences and oscillator strengths are obtained from dipole matrix elements between Kohn–Sham eigenstates (Supporting Information). Such an approximation has been theoretically justified^{12a} and found to work quite well to describe the electronic excitations of large clusters and nanoparticles.^{12b,c}

A schematic description of the electronic structure for the noninteracting and interacting dye/nanoparticle systems is reported in Figure 2. We previously found that inclusion of solvation effects was essential for a correct description of the excitation spectrum of Ru(II)-polypyridyl dyes.¹³ In the present case, solvation is essential also for stabilizing the $[\text{Fe}(\text{CN})_6]^{4-}$ dye and the $[\text{Fe}(\text{CN})_6]^{4-}/\text{TiO}_2$ complex. Furthermore, solvation appears to influence the molecular absorption geometry, stabilizing the monodentate configuration reported in Figure 1 with respect to a bidentate structure (Supporting Information) that is favored in a vacuum. A monodentate coordination mode has also been suggested by IR^{14a} and Raman spectroscopic data.^{14b} Thus, in the following, only results for the monodentate configuration in water solution are presented. As shown by Figure 2, the lineup of the noninteracting dye and nanoparticle energy levels is such that the highest occupied states of the dye form two groups of Fe t_{2g} and CN based orbitals that lie within the TiO_2 band gap. This picture remains qualitatively unchanged for the interacting $[\text{Fe}(\text{CN})_6]^{4-}/\text{TiO}_2$ system, even though shifts in the energy levels take place, Figure 2. For the bare $\text{Ti}_{38}\text{O}_{76}$ cluster, a HOMO–LUMO gap of 3.78 eV is computed, with a TDDFT lowest transition of 3.20 eV. The latter value is only slightly smaller than typical band gaps of TiO_2 nanoparticles a few nm in size.^{3,15} For the isolated $[\text{Fe}(\text{CN})_6]^{4-}$ dye, we compute a HOMO energy of -4.40 eV, i.e., ~ 1.6 eV below the isolated nanoparticle

[†] ISTM.

[‡] Princeton University.

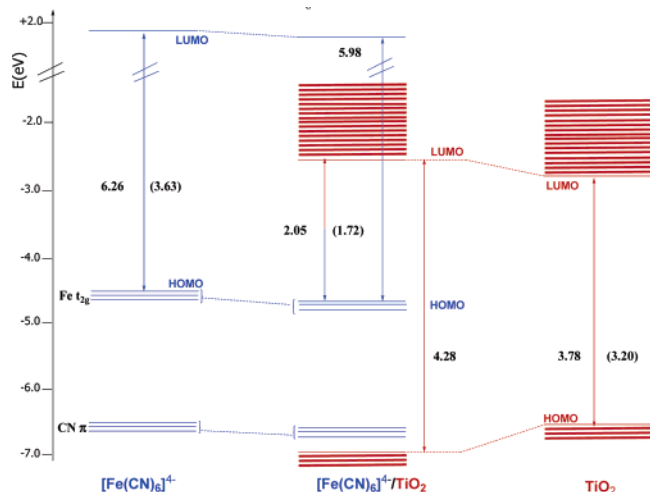


Figure 2. G03/B3LYP energy levels (eV) of the noninteracting $[\text{Fe}(\text{CN})_6]^{4-}$ (left) and TiO_2 (right) and interacting $[\text{Fe}(\text{CN})_6]^{4-}/\text{TiO}_2$ (middle) systems in water solution. Blue (red) colors refer to states that are mostly localized on the dye (nanoparticle). Values in parentheses refer to TDDFT excitation energies.

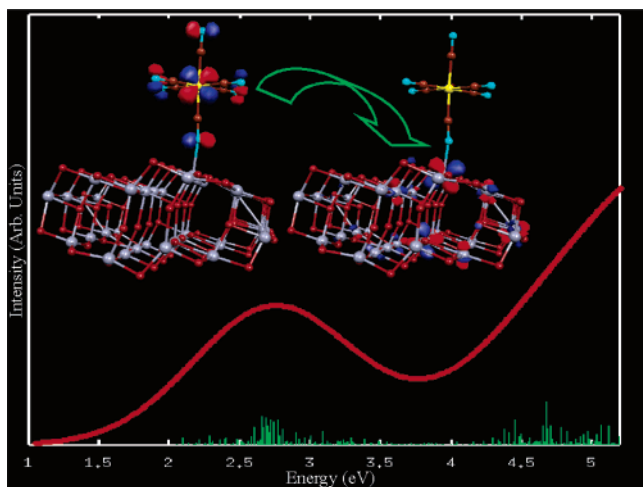


Figure 3. Calculated optical absorption spectrum of $[\text{Fe}(\text{CN})_6]^{4-}/\text{TiO}_2$. Two of the orbitals involved in the transitions that maximally contribute to the intensity of the MPCT band are also shown.

LUMO, in fairly good agreement with known lineups of semiconductor band edges and solution redox potentials.¹ Moreover, TDDFT yields a lowest excitation of 3.63 eV, consistent with the experimentally observed weak absorption band at ~ 3.85 eV for $[\text{Fe}(\text{CN})_6]^{4-}$ in solution.¹⁶

Turning to the interacting system, the HOMO–LUMO gap (2.05 eV), and correspondingly the TDDFT lowest excitation (1.72 eV), are drastically reduced with respect to those of the noninteracting systems. Inspection of the energy levels of the $[\text{Fe}(\text{CN})_6]^{4-}/\text{TiO}_2$ system reveals that the six HOMOs are very similar to those of the isolated $[\text{Fe}(\text{CN})_6]^{4-}$ molecule, whereas the lowest unoccupied states are localized on the cluster. Dye unoccupied states lie at much higher energies within the TiO_2 conduction band. The spectrum, calculated by the approximate procedure outlined above, exhibits a band at 2.75 eV, i.e., only 0.2 eV red-shifted with respect to the experiment,^{2,3} and well below the onset of the nanoparticle interband transitions computed at ~ 4.3 eV, Figure 3. All the transitions composing this low-energy feature are found to originate from the set of $\text{Fe } t_{2g}$ dye HOMOs to unoccupied TiO_2 states, with no contributions from the lower set of CN-based dye levels or from

unoccupied dye states. Two of the orbitals involved in the series of the most intense transitions composing this band are shown as insets in Figure 3, and allow us to confirm the assignment of the low-energy band as a MPCT transition. Moreover, the final states that maximally contribute to the intensity of the MPCT band are found to be largely localized on the $\text{Ti}(\text{IV})$ atom to which the dye molecule is coordinated, with some weaker contributions from the neighboring Ti atoms.

In conclusion, on the basis of DFT and TDDFT calculations we have provided a detailed characterization of the electronic structure and absorption spectrum of the prototypical $[\text{Fe}(\text{CN})_6]^{4-}/\text{TiO}_2$ system. Our results show that a direct charge injection process from an occupied dye molecular state to a nanoparticle excited state localized on few Ti atoms takes place in this system, in agreement with recent experimental evidence.

Acknowledgment. This work was partially supported by NSF through Grant CHE-0121432.

Supporting Information Available: Optimized structures and computational details (PDF). This material is available free of charge via the Internet at <http://pubs.acs.org>.

References

- (1) (a) O'Regan, B.; Gratzel, M. *Nature* **1991**, *353*, 737. (b) Rehm, J. M.; McLendon, G. L.; Nagasawa, Y.; Yoshihara, K.; Moser, J.; Gratzel, M. *J. Phys. Chem. B* **1996**, *100*, 9577. (c) Hagefeldt, A.; Gratzel, M. *Chem. Rev.* **1995**, *95*, 49. (d) Gratzel, M. *Nature* **2001**, *414*, 338–344.
- (2) (a) Yang, M.; Thompson, D. W.; Meyer, G. J. *Inorg. Chem.* **2000**, *39*, 3738. (b) Yang, M.; Thompson, D. W.; Meyer, G. J. *Inorg. Chem.* **2002**, *41*, 1254.
- (3) Khoudiakov, M.; Parise, A. R.; Brunshwig, B. S. *J. Am. Chem. Soc.* **2003**, *125*, 4637.
- (4) (a) Persson, P.; Bergstrom, R.; Lunell, S. *J. Phys. Chem. B* **2000**, *104*, 10348. (b) Rego, L. G. C.; Batista, V. S. *J. Am. Chem. Soc.* **2003**, *125*, 7989. (c) Stier, W.; Prezhdo, O. V. *J. Phys. Chem. B* **2002**, *106*, 8047. (d) Vittadini, A.; Selloni, A.; Rotzinger, F. P.; Gratzel, M. *J. Phys. Chem. B* **2000**, *104*, 1300.
- (5) Car, R.; Parrinello, M. *Phys. Rev. Lett.* **1985**, *55*, 2471.
- (6) Perdew, J. P.; Burke, K.; Ernzerhof, M. *Phys. Rev. Lett.* **1996**, *77*, 3865.
- (7) (a) Pasquarello, A.; Laasonen, K.; Car, R.; Lee, C.; Vanderbilt, D. *Phys. Rev. Lett.* **1992**, *69*, 1982–1985. (b) Giannozzi, P.; De Angelis, F.; Car, R. *J. Chem. Phys.* **2004**, *120*, 5903.
- (8) *Gaussian 03*, revision B.04; Frisch, M. J.; Trucks, G. W.; Schlegel, H. B.; Scuseria, G. E.; Robb, M. A.; Cheeseman, J. R.; Montgomery, J. A., Jr.; Vreven, T.; Kudin, K. N.; Burant, J. C.; Millam, J. M.; Iyengar, S. S.; Tomasi, J.; Barone, V.; Mennucci, B.; Cossi, M.; Scalmani, G.; Rega, N.; Petersson, G. A.; Nakatsuji, H.; Hada, M.; Ehara, M.; Toyota, K.; Fukuda, R.; Hasegawa, J.; Ishida, M.; Nakajima, T.; Honda, Y.; Kitao, O.; Nakai, H.; Klene, M.; Li, X.; Knox, J. E.; Hratchian, H. P.; Cross, J. B.; Adamo, C.; Jaramillo, J.; Gomperts, R.; Stratmann, R. E.; Yazyev, O.; Austin, A. J.; Cammi, R.; Pomelli, C.; Ochterski, J. W.; Ayala, P. Y.; Morokuma, K.; Voth, G. A.; Salvador, P.; Dannenberg, J. J.; Zakrzewski, V. G.; Dapprich, S.; Daniels, A. D.; Strain, M. C.; Farkas, O.; Malick, D. K.; Rabuck, A. D.; Raghavachari, K.; Foresman, J. B.; Ortiz, J. V.; Cui, Q.; Baboul, A. G.; Clifford, S.; Cioslowski, J.; Stefanov, B. B.; Liu, G.; Liashenko, A.; Piskorz, P.; Komaromi, I.; Martin, R. L.; Fox, D. J.; Keith, T.; Al-Laham, M. A.; Peng, C. Y.; Nanayakkara, A.; Challacombe, M.; Gill, P. M. W.; Johnson, B.; Chen, W.; Wong, M. W.; Gonzalez, C.; Pople, J. A.; Gaussian, Inc.: Pittsburgh, PA, 2003.
- (9) Becke, A. D. *J. Chem. Phys.* **1993**, *98*, 5648.
- (10) (a) Watchers, J. H. *J. Chem. Phys.* **1970**, *52*, 1033. (b) Binkley, J. S.; Pople, A. J.; Herbe, W. J. *J. Am. Chem. Soc.* **1980**, *102*, 939.
- (11) (a) Cossi, M.; Barone, V. *J. Chem. Phys.* **2001**, *115*, 4708. (b) Cossi, M.; Rega, N.; Scalmani, G.; Barone, V. *J. Comput. Chem.* **2003**, *24*, 669.
- (12) (a) Savin, A.; Umrigar, C. J.; Gonze, X. *Chem. Phys. Lett.* **1998**, *288*, 391. (b) Williamson, A. J.; Grossman, J. C.; Hood, R. Q.; Puzder, A.; Galli, G. *Phys. Rev. Lett.* **2002**, *89*, 196803. (c) Matxain, J. M.; Mercero, J. M.; Fowler, J. E.; Ugalde, J. M. *J. Am. Chem. Soc.* **2003**, *125*, 9494.
- (13) (a) Fantacci, S.; De Angelis, F.; Selloni, A. *J. Am. Chem. Soc.* **2003**, *125*, 4381. (b) De Angelis, F.; Fantacci, S.; Selloni, A. *Chem. Phys. Lett.* **2004**, *389*, 204. (c) Fantacci, S.; De Angelis, F.; Wang, J.; Bernhard, S.; Selloni, A. *J. Am. Chem. Soc.* **2004**, *126*, 9715. (d) Fantacci, S.; De Angelis, F.; Sgamellotti, A.; Re, N. *Chem. Phys. Lett.* **2004**, *396*, 43.
- (14) (a) Ghosh, H. N.; Asbury, J. B.; Weng, Y.; Lian, T. *J. Phys. Chem B* **1998**, *102*, 10208. (b) Blackburn, R. L.; Johnson, C. S.; Hupp, J. T. *J. Am. Chem. Soc.* **1991**, *113*, 1060.
- (15) Weng, Y. X.; Wang, Y. Q.; Asbury, J. B.; Ghosh, H. N.; Lian, T. *J. Phys. Chem B* **2000**, *104*, 93.
- (16) Shirom, M.; Stein, G. *J. Chem. Phys.* **1971**, *55*, 3372.

JA045152Z